2288 *Biochemistry* **2010,** *49,* 2288–2296
DOI: 10.1021/bi902121z

BIOCHEMISTRY
including biophysical chemistry & molecular biology
*Article*

# Temperature-Sensitive Reaction of a Photosensor Protein YcgF: Possibility of a Role of Temperature Sensor[†]

Yusuke Nakasone,[‡] Taka-aki Ono,[§] Asako Ishii,[∥] Shinji Masuda,[⊥] and Masahide Terazima*[,‡]

[‡]*Department of Chemistry, Graduate School of Science, Kyoto University, Kyoto 606-8502, Japan,* [§]*Department of Biomolecular Functional Engineering, Faculty of Engineering, Ibaraki University, Ibaraki 316-8511, Japan,* [∥]*Toin Human Science and Technology Center, Toin University of Yokohama, 1614 Kurogane-cho, Aoba-ku, Yokohama 225-8502, Japan, and* [⊥]*Center for Biological Resources and Informatics, Tokyo Institute of Technology, Yokohama 226-5801, Japan*

*Received December 10, 2009; Revised Manuscript Received January 29, 2010*

ABSTRACT: The spectrally silent photoreaction of a blue light sensor protein YcgF, composed of the N-terminal BLUF domain and the C-terminal EAL domain, was investigated by the time-resolved transient grating method. Comparing photoinduced reactions of full-length YcgF with that of the BLUF−linker construct, it was found that a major conformation change after photoinduced dimerization is predominantly localized on the EAL domain. Furthermore, the photoinduced conformational change displayed significant temperature dependence. This result is explained by an equilibrium of reactive and nonreactive YcgF species, with the population of photoreactive species decreasing as the temperature is lowered in the dark state. We consider that the dimer form is the nonreactive species and it is the dominant species at lower temperatures. The temperature sensitivity of the photoreaction of YcgF suggests that this protein could have a biological function as a temperature sensor as well as behaving as a light sensor.

Sensor proteins in organisms perform the essential role of detecting external environmental conditions that is vital for their survival. External stimuli induce changes in conformation, aggregation state, and/or intermolecular interaction of sensor proteins. These changes are communicated to a downstream domain or protein partner triggering a biological response. In order to understand the molecular mechanism of a biological response, it is essential to reveal the involved reaction scheme. Furthermore, it could be possible that clarification of the reaction scheme involved in sensor protein responses may allow discovery of other functions of these proteins. In this study, we have investigated the photochemical reaction of a light sensor protein YcgF at the molecular level. The reaction scheme of YcgF is presented. Interestingly, the reaction exhibits a significant temperature dependence suggesting that YcgF also has a role as a temperature sensor.

The YcgF protein from *Escherichia coli* is composed of an N-terminal BLUF[1] [sensors of *b*lue *l*ight *u*sing *F*AD (flavin adenine dinucleotide)] domain and a C-terminal EAL domain, which contains an abundance of the amino acids glutamate (E), alanine (A), and leucine (L) (*1*, *2*). The BLUF domain contains about 100 amino acid residues with sequence similarity and acts as a blue light receptor. BLUF domains are widespread among prokaryotic and eukaryotic microorganisms; e.g., AppA, PAC, SyPixD, TePixD, and BlrB (*3*−*12*). The EAL domain has been shown to hydrolyze cyclic diguanosine monophosphate (c-di-GMP), which is a regulatory signaling molecule for various biological events (*1*). Recently, it was reported that YcgF could not be involved in c-di-GMP metabolism but acts by direct protein−protein interaction with the MerR-like repressor YcgE to release it from its operator DNA in a blue light-dependent manner (*13*).

It has been shown that the photochemistry of BLUF domains has a common feature; i.e., signaling state formation is accompanied by a red shift of the UV−visible absorption spectrum caused by hydrogen bond rearrangement around FAD (*5*, *7*, *9*, *11*, *14*−*19*). Since YcgF shows a similar spectral shift, the local change in hydrogen bonding should be the initial step of signal transduction (*1*, *20*). The subsequent reaction has not been determined using UV−visible light absorption detection (a half-decay time of red-shifted species is about 2 min for YcgF). We have elucidated the subsequent chemistry of YcgF by monitoring changes in the volume and diffusion coefficient (*D*) (*21*). It was found that the structural change (13 $\mu$s) and following protein−protein association reaction (2 ms at a protein concentration of 700 $\mu$M) are induced by the photoexcitation of YcgF. The dimerization reaction induced significant conformational change that affects the diffusion process (diffusion-sensitive conformation change (DSCC)). Interestingly, the linkage between BLUF and EAL domains is predicted to involve a predominantly helical segment (called a J-helix). Recent NMR measurements showed that photoinduced conformational changes occur within a construct of BLUF and linker domains (*22*). Therefore, information of the local change around FAD is transmitted to the EAL region through either the linker or the interaction between the BLUF domain and linker. These

[†]This work was supported by Grant-in-Aid for Scientific Research (A) (No. 18205002), Grant-in-Aid for Scientific Research on Innovative Areas (20107003), and Scientific Research on Innovative Areas (research in a proposed research area) (20107003) from the Ministry of Education, Science, Sports, and Culture in Japan.

*Corresponding author. Phone: +81-75-753-4026. Fax: +81-75-753-4026. E-mail: mterazima@kuchem.kyoto-u.ac.jp.

[1]Abbreviations: BLUF, blue light using FAD; c-di-GMP, cyclic diguanosine monophosphate; DSCC, diffusion-sensitive conformational change; EAL, glutamate(E) alanine(A) leucine(L); *E. coli*, *Escherichia coli*; FAD, flavin adenine dinucleotide; LOV, light, oxygen, and voltage; NMR, nuclear magnetic resonance; phot1, phototropin 1; phot2, phototropin 2; SEC, size-exclusion chromatography; TG, transient grating.

 Published on Web 02/08/2010 

interactions and reactions should have a crucial role in regulating the activity of the EAL domain and hence should be essential for their signal transduction.

However, the reaction scheme remains unclear; e.g., which domain, BLUF or EAL, is responsible for the conformational change? To elucidate the reaction scheme in more detail, we investigated the reaction dynamics of the C-terminal truncated construct, which includes only BLUF and linker regions, by transient grating (TG) measurement. The observed TG signals showed only minor volume change with a time constant of 30 $\mu$s, and diffusion signals were not detected. This indicates that the photoinduced dimerization process does not occur in the BLUF−linker construct.

Furthermore, we found a drastic temperature effect on the photoinduced dimerization; the TG signal intensity that represents diffusion change strongly depends on the temperature. This result indicates that reactive and nonreactive YcgF species exist and the population of photoactive species decreases as the temperature is decreased in the dark state. The temperature dependence of the gel chromatography elution profile under dark conditions shows that the dimer dominates at lower temperatures. This indicates that the dimer form does not undergo further association reactions upon photoexcitation. On the basis of the temperature sensitivity of the reaction, we propose that YcgF may behave like both a photosensor and a temperature sensor.

## MATERIALS AND METHODS

*Preparation of Recombinant BLUF Polypeptides*. The YcgF and BLUF−linker construct (1−148) expressed in *E. coli* was prepared using the same method described previously (*20*). The protein was purified using a His-Bind resin (Novagen) and dialyzed against a buffer containing 2 mM NaCl, 2 mM $MgCl_2$, and 20 mM Tris-HCl (pH 8.0). The purified protein was stored at −80 °C until use. Protein concentrations were determined from the absorbance at 450 nm using the absorption coefficient of FAD (11.3 $mM^{-1}$ $cm^{-1}$).

*TG Measurement*. The experimental setup for the TG experiments was similar to that previously reported (*21*, *23*−*31*). In the TG experiments, a laser beam from a XeCl excimer laser-pumped dye laser (Lambda Physik Compex 102xc, Lumonics Hyper Dye 300; $\lambda$ = 465 nm) was split into two by a beam splitter and crossed inside a quartz sample cell (optical path length = 2 mm). The refractive index modulation (transient grating) created in the sample was probed by a diode laser (835 nm) as a Bragg diffracted signal (TG signal). The TG signal was detected by a photomultiplier tube (Hamamatsu R-928) and fed into a digital oscilloscope (Tektronix TDS-5054). The TG signal was averaged by a microcomputer to improve the signal-to-noise (S/N) ratio. The grating wavenumber ($q$) was varied by changing the crossing angle of the excitation beam. The repetition rate of the excitation beam was set at 0.01 Hz, and the solution was stirred after every shot of the excitation pulse for the TG experiments to avoid excitation of the photoproduct. The repetition rate was set as low as possible, particularly for low temperature measurements. Principles and theory are described in Supporting Information.

*Size-Exclusion Chromatography*. For size-exclusion chromatography, Superdex 200 5/150 GL (GE Healthcare, Germany) equilibrated with buffer [20 mM Tris-HCl (pH 8.0), 2 mM NaCl, and 2 mM $MgCl_2$] was used. At a flow rate of 0.5 mL $min^{-1}$ the elution profile was calibrated with glutamate dehydrogenase (290 kDa), lactate dehydrogenase (142 kDa), enolase (67 kDa), myokinase (32 kDa), and cytochrome *c* (12.4 kDa). The temperature dependence of the elution profile was measured at 278 and 293 K. Elution profiles were monitored with an AKTA purifier system (GE Healthcare) by detecting the absorption at 280 nm. Chromatography experiments were carried out in the dark. Calibrations were performed at each temperature before measurement of the YcgF solution.

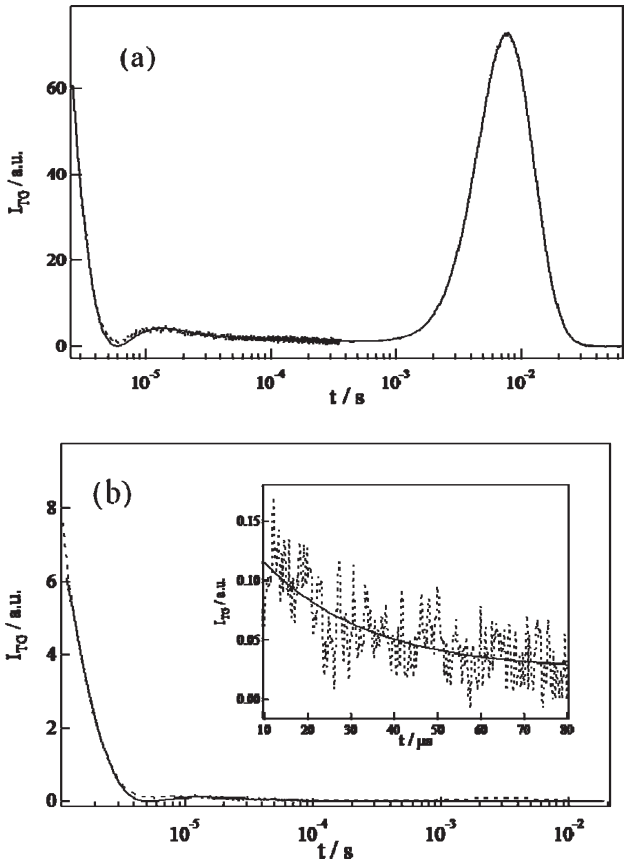


FIGURE 1: (a) A typical TG signal (broken line) of YcgF after photoexcitation in 20 mM Tris-HCl, 2 mM NaCl, and 2 mM $MgCl_2$ (pH 8.0) buffer at a concentration of 700 $\mu$M, $q^2 = 3.3 \times 10^{12}$ $m^{-2}$ at 293 K. The fitting curve based on the time-dependent $D$ model (Supporting Information eq S-2) is shown as a smooth solid line. (b) A typical TG signal (broken line) of the BLUF−linker sample after photoexcitation in the same buffer at a concentration of 70 $\mu$M, $q^2 = 3.6 \times 10^{12}$ $m^{-2}$ at 293 K. The fitting curve based on biexponential function (eq 1) is shown as a solid line. The volume grating component is magnified in the inset plot with a linear time scale.

## RESULTS

*The Photoreaction of YcgF*. Before describing the temperature dependence of the YcgF photoreaction, the reaction scheme of YcgF upon photoexcitation should be clarified. To clarify the photochemical reaction of YcgF, the features of the TG signals of YcgF and the C-terminal truncated YcgF construct (BLUF−linker) at 293 K are examined initially. The TG signal after photoexcitation of intact YcgF initially decayed in the submicrosecond time range and showed two rise-decay components (Figure 1a). The temporal profile of the signal was analyzed in detail previously (*21*). The initial decay component and the subsequent weak decay component with a time constant of 13 $\mu$s were assigned to a thermal grating and to a volume grating reflecting the conformational change of the protein, respectively.

The magnitude of the volume change was calculated from the amplitudes of refractive index change $\delta n_v$ to be $+3.5 \pm 1.5$ mL/mol. The most notable feature of the TG signal was the strong rise-decay component that represents protein diffusion. We found that $D$ was time dependent, and the temporal profile was analyzed by a model of the time-dependent $D$ (Supporting Information eq S-2). $D$ decreased from $D_R = (8.3 \pm 0.2) \times 10^{-11}$ $m^2/s$ to $D_P = (3.8 \pm 0.2) \times 10^{-11}$ $m^2/s$ with a time constant of 2 ms at a concentration of 700 $\mu$M at 293 K. By comparing $D_R$ with other proteins, we found that the reactant existed as a monomer. From the concentration dependence of the reaction rate, we concluded that the reaction is the dimerization of YcgF:

$$2M \xrightarrow{h\nu} M* + M \rightarrow DI* \quad (A)$$

where M is the monomer of YcgF, M* is the photoexcited monomer, and DI* is the dimer that contains one excited M.

The observed decrease in $D$ upon dimer formation has two origins. First, the molecular volume increased by a factor of 2 upon dimerization leading to an increase in the molecular radius by a factor of $2^{1/3} = 1.26$. Hence, if the Stokes−Einstein relationship holds, one expects $D$ to decrease by 1.26. Here, we assumed that the effect of molecular shape change is negligibly small. This assumption is reasonable, because even if a molecule has an elongated shape with a ratio of $a/b = 2$ (a semimajor axis $a$ and a minor axis $b$), $D$ will decrease only a factor of 0.97 compared to that of a spherical molecule with the same volume, according to Perrin's equation (*32*, *33*). This factor is too small to explain the observed change ($D_R/D_P = 2.2$). There must be another contribution to the decrease in $D$: a conformational change in the protein leading to an enhanced interaction between solvent and protein (DSCC).

Here, it should be essential to answer a question: which part of YcgF causes the increase in the intermolecular interaction? To further understand the photoreaction of YcgF, a C-terminally truncated YcgF [BLUF−linker sample (M1-D148)], which contains the BLUF domain and the entire linker region except for the EAL domain (P145−K403), was investigated. This linker region is predicted to form a predominantly helical structure (*22*). A typical example of the observed TG signal of the BLUF−linker at a concentration of 70 $\mu$M and grating wavenumber of $q^2 = 3.8 \times 10^{12}$ $m^{-2}$ is shown in Figure 1b. The temporal profile was similar to that of YcgF until the submillisecond time range, but after this it was quite different. The signal decayed to the baseline and showed a single weak rise-decay profile without any diffusion peak. Since the first decay rate agreed with $D_{th}q^2$ ($D_{th}$ is the thermal diffusivity), the component was assigned to a thermal grating. The observed signal was expressed by the square of the biexponential function:

$$I_{TG}(t) = \alpha\{\delta n_{th} \exp(-D_{th}q^2t) + \delta n_{v'} \exp(-k_{v'}t)\}^2 \quad (1)$$

where $\delta n_{v'}(>0)$ is the amplitude and $k_{v'}$ is the rate constant of the species grating signal after the thermal grating signal. The lifetime of the second decay $k_{v'}^{-1}$ was determined to be 30 $\mu$s. Since the rate of this decay was independent of $q^2$, this component was attributed to the volume grating. Although similar dynamics were also observed for YcgF, the time constants were different (13 $\mu$s for YcgF and 30 $\mu$s for the BLUF−linker). The difference in these time constants indicated that the presence of the EAL domain affects this dynamic. Therefore, the initial conformational change of the $k_v$ phase of YcgF does not occur solely around the chromophore in the BLUF domain; the EAL domain is also involved. The volume change was determined to be $+0.9 \pm 0.3$ mL/mol. This is smaller than the value detected for YcgF ($+3.5 \pm 1.5$ mL/mol), providing further evidence that the EAL domain also undergoes conformational change upon photoexcitation of YcgF.

The most significant observation was that the diffusion peak was not observed for the BLUF−linker construct (Figure 1b). This result indicates that $D$ does not change upon the photoexcitation of the BLUF−linker, i.e., no dimer formation and no conformational change. Here we should note that the BLUF−linker is known to exist as a dimer in solution before photoexcitation, whereas intact YcgF exists as a monomer (*1*, *21*). On the basis of these facts, it is reasonable to consider that the dimerization site is the BLUF domain and this site is intermolecularly blocked by the dimer formation for the BLUF−linker sample. This blocking may be a cause of the lack of photoinduced dimerization reaction. On the other hand, for intact YcgF, the dimerization site is masked intramolecularly by the EAL domain so that it exists as a monomer in the dark. Upon photoexcitation of YcgF, the dimerization site is exposed, leading to dimer formation and subsequent DSCC. This suggests that the BLUF domain is the dimerization site for the BLUF−linker in the dark state and also for YcgF in the photoexcited state. In fact, it has been reported that many short BLUF proteins form oligomers; e.g., SyPixD and TePixD form decamers in crystals, and BlrB and AppA-BLUF form dimers (*10*, *12*, *16*, *17*). These facts suggest BLUF domains have a tendency to form oligomers due to strong intermolecular interactions. Previously, FTIR measurements were reported to show a change in the amide1 band for YcgF but not for the BLUF−linker construct (*20*). This indicates that the conformational change detected for YcgF that occurs in the EAL region is mainly triggered by dimerization. (It could be possible that the reaction of the BLUF domain without the EAL domain is different from that of the full-length protein. However, in this YcgF case, since the isolated BLUF domain showed the same spectral change with that of the intact protein and the volume change was also observed, we consider that the reaction of the BLUF domain is the same as that of the BLUF domain of the native protein.)

The initial conformation change exhibited as the volume changes occurs for both intact YcgF and the BLUF−linker sample. This common feature suggests that the BLUF−linker domain is mainly responsible for this change. Recently, NMR spectroscopy showed that the helix of the linker region is in contact with the BLUF core in the dark-adapted state, but this interaction is reduced in the light-adapted state for BlrB and Blrp1 (*34*, *35*). We suggest that the reaction with a time constant of 30 $\mu$s represents the dissociation process of the helix from the BLUF domain. However, since the rate and amplitude of the volume change associated with this reaction were different between BLUF−linker and YcgF, the EAL region is involved in this reaction. Therefore, upon the absorption of blue light, the change in the hydrogen-bonding network around FAD causes a change in the interdomain interaction between the BLUF and linker regions and results in the dissociation of the EAL domain from the BLUF core with a time constant of 13 $\mu$s. Consequently, intermolecular association takes place upon exposing the interaction site of the BLUF domain, resulting in a conformational change in the EAL region, which enhances the intermolecular interaction with solvents.

A conformational change that can alter interprotein interactions should be important for the signaling state formation of sensor proteins. This DSCC could be an essential process for the creation of the signaling state. Recently, it was reported that YcgF directly interacts with the MerR-like repressor YcgE and, in a blue light-dependent manner, releases it from the DNA, where YcgE specifically binds to the YcgZ promoter (*13*). The release was considered to be caused by an increase in the affinity of YcgF for YcgE upon blue light irradiation. Our results show that the intermolecular interaction of YcgF changes upon photoexcitation; it may be this change that results in the release of YcgE from its operator site.

*Temperature-Sensitive Photochemistry of YcgF.* In this study the most significant observation is that the photochemical reaction of YcgF is highly temperature dependent. Panels a and b of Figure 2 show the TG signals representing the molecular diffusion of YcgF at a range of temperatures between 283 and 308 K at $q^2 = 7.0 \times 10^{10}$ m$^{-2}$ at 700 $\mu$M. As the temperature is decreased, the signal profile changes drastically. The peak time of the diffusion signal shifts to a longer time range as the temperature decreases. Over a temperature range of 283−308 K, the most obvious change was a decrease in the diffusion peak intensity as the temperature was lowered. Below 298 K further temperature decreases resulted in a new rise-decay component at a longer time range which gradually increased in intensity. The origin of these temperature-dependent features should be understood consistently.

The reason for the small shift of the TG signal to a longer time range at lower temperatures is obvious. As the viscosity of the solution increases with decreasing temperature, the diffusion rate should slow. In fact, using the $D$ of the monomer and dimer (corrected for the viscosity and temperature based on the Stokes−Einstein relation), the observed TG signals can be accurately reproduced as shown below.

We next consider the origin of the decrease in the diffusion peak intensity in the temperature range of 308−283 K. The diffusion peak in the subsecond time range appears because $D$ changes upon photoreaction. To explain the decrease in the diffusion peak intensity at decreasing temperatures, there are two possibilities. First, if the dimerization rate slowed with decreasing temperature so that the rate became close to the protein diffusion time at this $q^2$, the dimer formation kinetics would overlap with the diffusion kinetics and the diffusion peak would weaken. We examined this possibility by considering the temporal profile. If the dimer formation kinetics are comparable to the diffusion signal, the temporal profile of the signal should not be reproduced by the biexponential function, but the time-dependent $D$ model (Supporting Information eq S-2) should instead be used. However, the excellent agreement of the calculated signal using a biexponential function (Supporting Information eq S-1) to the observed signal indicates that dimer formation was completed before the diffusion signal appeared. Therefore, we excluded this first possibility.

The second possibility is that if reactive and nonreactive species exist in equilibrium and the equilibrium constant depends on the temperature, the signal intensity of the diffusion peak should be temperature dependent. Here it should be noted that if photoexcitation does not lead to any change in $D$, the signal should not appear. What are the reactive and nonreactive species of this possible mechanism? The photoreaction of YcgF involves a conformational change caused by dimerization. It is plausible that if a dimer of YcgF already exists before photoexcitation

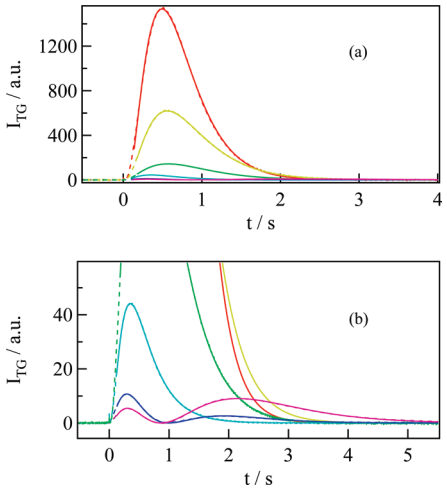


FIGURE 2: (a) Temperature dependence of the TG signal of YcgF (broken lines) at a concentration of 700 $\mu$M and $q^2 = 3.8 \times 10^{10}$ m$^{-2}$ (red, 308 K; yellow, 303 K; green, 298 K; cyan, 293 K; blue, 288 K; magenta, 283 K). (b) The signal intensities are enlarged to show the weak part of the signals. The lines of best fit based on three diffusion components (eq 2) are shown as solid lines.

(i.e., in the dark), photoinduced dimerization may be prevented. Hence, let us assume that the nonreactive species is a dimer of YcgF, and the dimer and monomer are in equilibrium in the dark. Later, this equilibrium was examined by size-exclusion chromatography and was found to be a plausible explanation for the variation in intensity of the diffusion peak.

What will happen if we photoexcite the dimer? If the $D$ of the dimer that consists of two ground state monomers (DI) is different from that of the dimer with one photoexcited monomer (DI*), the difference should appear in the TG signal. We suggest that the new peak which appeared at low temperature represents this component. The presence of a monomer−dimer equilibrium is supported by a quantitative analysis of the TG profile as follows. Below 288 K (Figure 2b), a new component became apparent at a longer time range. Since the time range of the signal depends on $q^2$, the observed signals represent molecular diffusion processes. The diffusion signal was expressed by the equation:

$$I_{TG}(t) = \alpha\{-\delta n_R \exp(-D_R q^2 t) + \delta n_P \exp(-D_P q^2 t) + \delta n_3 \exp(-D_3 q^2 t)\}^2 \quad (2)$$

where $D_3$ is a diffusion coefficient of the new species ($D_R > D_P > D_3$) at low temperature and $\delta n_3$ is the initial refractive index change of this component. To reproduce the TG signal, $\delta n_3$ should be a negative value. The negative sign of $\delta n_3$ indicates that these components represent the diffusion of the reactant. The diffusion coefficients of each component were determined using eq 2 (corrected for viscosity and temperature based on the Stokes−Einstein relationship and $D_3 = (3.4 \pm 0.2) \times 10^{-11}$ m/s$^2$ at 293 K). Since $D_3$ is similar to $D_P$, this component was attributed to the dimer as a reactant (DI). Based on these results, a diffusion coefficient change also occurred in the photoreaction of DI. The change is minor, which suggests that the product of this reaction (DI*) should have a similar conformation to that of DI.

$$\mathrm{DI} \xrightarrow{h\nu} \mathrm{DI}* \quad (B)$$

Since the diffusion coefficient change of this reaction is very small compared with that of reaction A, the signal intensity should be very weak and easily masked by the strong signal of the dimerization reaction above 293 K.

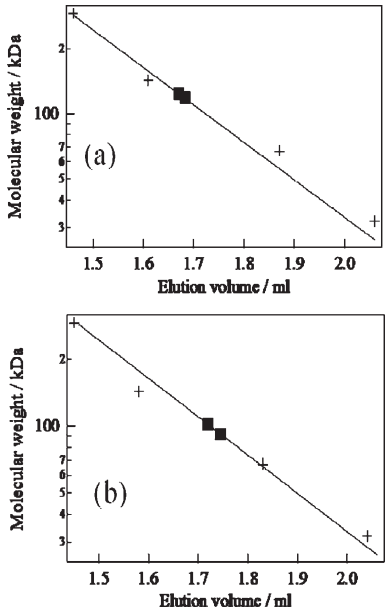


FIGURE 3: Concentration dependence of the elution peak position of YcgF at 40 and 400 $\mu$M (initial concentrations) at (a) 278 K and (b) 293 K. The column was equilibrated with buffer (20 mM Tris-HCl (pH 8.0), 2 mM NaCl, and 2 mM $MgCl_2$). The elution peak position was plotted on the calibration curve by measuring the absorption at 280 nm. Filled squares and cross symbols indicate the position of the elution peak for YcgF at each concentration and of the marker proteins, respectively. Chromatography experiments were carried out in the dark.

As confirmation of the above analysis, we determined that the magnitude of $\delta n$ of the product ($\delta n_P$) was independent of temperature. This is consistent with the above mechanism because the total amount of the product DI* should be temperature independent.

*Dimer−Monomer Equilibrium*. In order to observe the monomer−dimer equilibrium by an independent method, we measured the elution profiles of YcgF by size-exclusion chromatography. Panels a and b of Figure 3 show the plots of the elution peak position of YcgF to the calibration curve measured in the dark at 278 and 293 K, respectively. At 278 K (Figure 3a), the peak position depended slightly on the concentration. When the YcgF concentration was increased from 40 to 400 $\mu$M, the peak shifted to higher molecular mass (MW) (MW of YcgF is 47 kDa as a monomer). The apparent MW determined from a plot on the calibration curve shifted from 119 to 122 kDa by increasing the concentration. When the temperature was increased from 278 to 293 K, the peak shifted to smaller MW, and the peak became more sensitive to concentration. The apparent MW shifted from 90 to 101 kDa as the concentration was increased. This shift could be explained in terms of monomer−dimer or dimer−trimer equilibrium. Although the observed MW at the lower concentration (90 kDa) is larger than that of the monomer, we consider that this shift reflects the monomer−dimer equilibrium on the basis of the following reasons. First, the $D$ value of the reactant from the TG measurement is consistent with that of the monomer as reported before (*21*). Hence, the dominant reactive species should be the monomer. Second, the elution behavior in SEC is dependent on hydrodynamic properties of the molecule, and the reported MW's determined by the SEC were sometimes larger than that of expected values. The reason could be due to a fact that globular proteins, which tend to be eluted faster than nonglobular proteins, are usually selected as the maker proteins. In fact, a paper on YtvA, which is a similar multidomain protein as YcgF, showed 1.6 times larger molecular mass than expected (*36*). In another example, the homopentamer of hemoporin eluted at the same time or a little faster than a globular protein hemocyanin, even though its molecular mass is smaller (*37*). Third, the MW from the SEC measurement did not depend on the concentration so much at low temperature (278 K). This fact suggested one of species in the equilibrium scheme is dominant at this temperature. The value of this species (122 kDa) is smaller than that of the trimer (141 kDa). Considering the above fact (MW's from SEC are sometimes larger than the true value(*36*, *37*)), we attributed this species to the dimer not the trimer. If this assignment is correct, the species having a smaller MW should be attributed to the monomer. Therefore, we concluded that the monomer−dimer equilibrium exists in the dark state, although dimer−trimer equilibrium cannot be excluded completely. However, the other experimental data shown in the previous section and analyses presented below are consistent with the assignment of the monomer−dimer equilibrium.

The elution profile consisted of a single peak (data not shown). If the monomer and dimer exist as stable isomers without time to equilibrate over the elution period, two peaks corresponding to the monomer and the dimer should be observed. On the contrary, if the equilibrium process is fast, an averaged molecular mass of the two isomers is expected. Although it is difficult to estimate the lower limit of the equilibrium rate for observing a single peak, the single concentration-dependent peak indicated that the monomer and the dimer form an equilibrium much faster than 15 min (elution time).

From these observations, we conclude that there is a temperature-dependent equilibrium between the monomeric and dimeric forms of YcgF and only the monomer can undergo photoinduced dimerization. Since the concentration at the detector position could not be determined during the chromatography experiment, the equilibrium constant could not be determined from the peak position. However, since the TG signal should be expressed by a superposition of reactions A and B by the biexponential functions, the equilibrium could be investigated quantitatively using the TG method at various temperatures (see Supporting Information, S-2). The calculated fraction of the photoreaction due to the monomer $f_M$ was plotted against temperature (Figure 4a). Figure 4b shows a plot of ln $K$ vs temperature. From the slope of the plot and the intercept with the ordinate, the differences of the enthalpy $\Delta H$ and the entropy $\Delta S$ between the monomer and dimer were determined to be $96 \pm 9$ kJ (mol of dimer)$^{-1}$ and $313 \pm 28$ J (mol of dimer K)$^{-1}$, respectively.

It may be interesting to observe the light effect on their elution profile. However, since the gels are white (highly light scattering) and the half-decay time of the light adapted state (2 min) is much shorter than the elution time, it was difficult to detect the signal under the light condition. We will consider this type of experiment in future.

*Temperature-Dependent Volume Change*. We also investigated the temperature dependence of the volume change associated with the initial conformation change with a time constant of 13 $\mu$s ($\Delta V_1$) and with the DSCC ($\Delta V_2$). The TG signal and $\Delta V_1$ are presented in Supporting Information Figure S-1. It clearly shows that the magnitude of $\Delta V_1$ is small and the temperature dependence is minor. These results may indicate that the temperature dependence of $\Delta V_1$ associated with reactions A and B are similar. Since this process is considered to be a

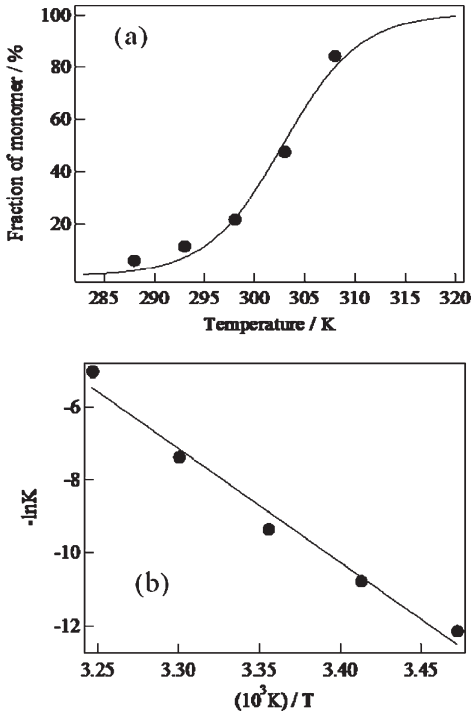


FIGURE 4: (a) Fraction of monomer determined from TG signals at various temperatures. (b) Plot showing the equilibrium constant versus the inverse of temperature.

conformational change in the BLUF domain, the similar trends observed for reactions A and B are understandable.

In addition, the TG signals representing the volume change associated with the dimerization process were measured, and $\Delta V_2$ were calculated (Supporting Information Figure S-2). We found that $\Delta V_2$ decreased with decreasing temperature. Since this volume change originated from the dimerization process and the dimer species cannot undergo further association upon photoexcitation, this volume change mostly comes from the reaction of monomeric species. Hence, we can estimate the value of volume change per monomer by dividing the value of the observed $\Delta V_2$ by the fraction of monomer in the initial state. The temperature dependence of $\Delta V_2$ per monomer is shown in Figure 5. We found that the volume change was sensitive to temperature. From the slope of the plot, $V\Delta\alpha_{th}$ for this reaction was determined to be $-0.40$ ($\pm 0.06$) $cm^3 mol^{-1} K^{-1}$. Since the thermal expansion coefficient is related to the cross-correlation of the entropy and volume fluctuations (*38*, *39*), this suggests that the conformational fluctuation is suppressed by the dimerization process. The difference of $V\Delta\alpha_{th}$ between the folded and unfolded metmyoglobin (metMb) was reported to be 2.4 $cm^3 mol^{-1} K^{-1}$ (*40*). In a dissociation process of the J-helix from the LOV2 domain of *Arabidopsis* phot2, the change in $V\Delta\alpha_{th}$ was measured to be $+0.09\ cm^3 mol^{-1} K^{-1}$ (*31*). Comparing with these values, we consider that the suppression effect by the dimerization of YcgF is relatively large.

## DISCUSSION

On the basis of the experimental data obtained from TG experiments, we propose the photoreaction scheme of YcgF. The experimental findings we should particularly consider are as follows:

(1) The monomer and dimer forms of YcgF are in a temperature-dependent equilibrium in the dark.

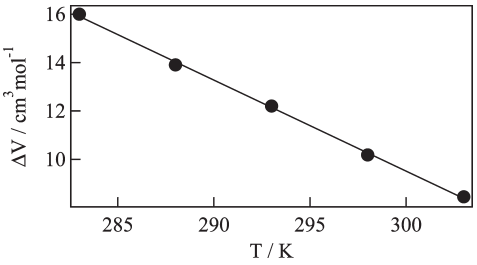


FIGURE 5: Temperature dependence of the volume change associated with dimerization per monomer determined from the TG signal at a concentration of 700 $\mu$M ($q^2 = 1.6 \times 10^{11}\ m^{-2}$).

(2) Photoexcitation of the monomer leads to dimerization, forming DI*. Before dimer formation of the photoexcited monomer, the *D* change is negligible. Hence, changes in *D* are mostly associated with the dimerization reaction.

(3) The *D* of the ground state dimer (DI) is much smaller than the *D* of the monomer but similar to that of DI*. This indicates that dimerization induces the DSCC, which is consistent with the above point.

(4) The small change in *D* upon reaction of the dimer indicates that the change in dimer structure upon photoexcitation is small. Furthermore, the *D* of the photoproduct from DI is the same as that of the photoproduct from reaction of M. This implies that the product is the same regardless of the reactants (monomer or dimer).

(5) Since the BLUF−linker construct exists as a dimer in solution in the dark and upon photoexcitation the BLUF−linker does not undergo further association, the photoinduced dimerization site could be the same as that of the dimer in the dark and is located in the BLUF domain. Also, the dimer of YcgF could not undergo further association reactions upon photoexcitation. This may indicate that the dimerization site in the dark-adapted state is the same as that in the light-adapted state; i.e., YcgF forms a dimer through BLUF−BLUF interactions.

(6) Photoexcitation of the BLUF−linker construct showed a conformational change (a volume change over 30 $\mu$s), although the magnitude of the change is smaller than that observed for YcgF. This change was assigned as the dissociation of the J-helix from the BLUF core. Similarly, in the case of YcgF, the EAL domain also dissociates from the BLUF core upon light irradiation.

(7) We propose that the dimerization site is located in the BLUF domain. However, intact YcgF can exists as a monomer. Therefore, we consider that the EAL domain might prevent dimerization in the dark. The interdomain interactions may use the same surfaces of the BLUF domain for both BLUF−BLUF and BLUF−EAL interactions. In the crystal structure of BlrB, the dimer interface is made up of $\beta$-strands which are not involved in the BLUF−linker interaction (*11*). Therefore, these $\beta$-strands should contribute to the association of the BLUF and EAL domains in YcgF. On the basis of these results, we propose that dissociation of the linker leads to dissociation of the BLUF and EAL domains, permitting the subsequent dimerization of YcgF. We consider that the monomer−dimer equilibrium in the dark indicates the equilibrium between the associated and dissociated BLUF−linker species. The dissociated species can easily form a dimer via interactions between exposed surface areas.

On the basis of these observations, we propose the reaction scheme of YcgF shown in Figure 6.

Under *in vitro* experimental conditions, YcgF is photoexcited to form the dimer (DI*). In this study, we used the YcgF sample

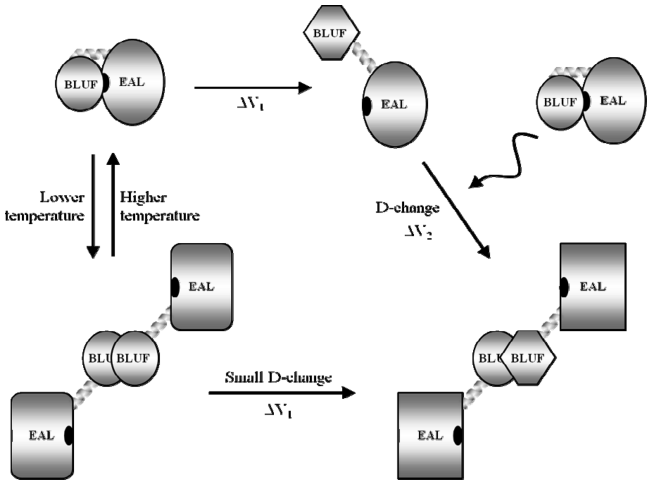


FIGURE 6: Schematic illustration of the photochemical reaction dynamics of YcgF. The BLUF and EAL domains are connected by the linker (α-helix). The monomer and dimer are in equilibrium in the dark. After creation of the red-shifted species, the photoexcited monomer changes conformation with a time constant of 13 $\mu$s at 293 K, indicated by the increase of the partial volume. With a time constant of 2 ms at a concentration of 700 $\mu$M, two monomers dimerize and the conformation changes, revealed by changes in the diffusion coefficient.

with a concentration of 700 $\mu$M, which could be higher than that of the intracellular condition. However, in our previous paper, we reported the dimerization rates at various concentrations (*21*). According to the result, the dimeriazation rate is 20 ms even at a concentration of 70 $\mu$M. Therefore, we believe this dimerization reaction occurs even at a diluted condition and could be relevant for *in vivo* function. Furthermore, under crowding condition such as in the cell, the dimer formation is usually favorable (unpublished work). We will further investigate the dimerization reaction under the crowding condition.

On the basis of present experimental data and previous reports, we suggest that photoinduced dissociation of the linker region results in dissociation of the BLUF and EAL domains. Consequently, YcgF dimerizes via a BLUF−BLUF interaction through exposure of the intermolecular interaction site. Moreover, this dimerization process leads to further conformational change in the EAL region which strengthens the solvent interaction and thus decreases *D* significantly. Recently, a similar oligomerization-dependent signal transduction mechanism was reported for another BLUF protein SyPixD from *Synechocystis*. In solution, SyPixD has been reported to exist as a trimer or a tetramer(*7*) or a dimer (*41*), and it forms a decamer when it interacts with PixE (the response regulator protein) in the dark (*41*). This indicates that SyPixD needs to form the decamer to interact with the effector protein PixE and this state is stabilized by the complex formation with PixE. In the case of TePixD, Tanaka et al. reported that the equilibrium between the pentemeric state and decameric state exists in solution and the photoexcitation of only the decameric form leads to a significant conformational change (*42*). These observations indicate that the oligomeric state is important in controlling the light signal transduction. Therefore, it is reasonable to consider that the dimeric form of YcgF and conformational change of the EAL domain are essential for its affinity to YcgE and consequently signal transduction.

Recently, Barends et al. reported the crystal structure of Blrp1, a multidomain protein consisting of the N-terminal BLUF domain and C-terminal EAL domain, and it forms a dimer in the dark (*43*). Interestingly, in its dimer, the C-terminal helices of the BLUF domains contact with the EAL domains of the other monomers. Since the crystallization was performed at 277 K by using a high-concentrated sample (19 mg $mL^{-1} \sim 400$ $\mu$M), the observed dimeric form is consistent with our results. However, the interface of the dimeric structure is different from what we expected for YcgF in this study; i.e., the dimer is formed by the BLUF−BLUF interaction for YcgF. This difference may reflect their different functions; Blrp1 has a c-di-GMP hydrolytic activity without any interprotein interaction. We speculate that Blrp1 forms such a compact dimer to enhance their efficiency via the quaternary structure-mediated EAL activation (*43*). In the case of YcgF, however, it might be better to form an open structure to interact with the target protein YcgE.

An important observation here is that the temperature also changes the protein intermolecular interactions (their oligomeric states), which could be important for the biological response. This observation leads to an interesting suggestion: YcgF not only is a photosensor but also has a function as a temperature sensor. Interestingly, Tschowri et al. showed that a low temperature (16 °C) alone can trigger YcgF-mediated relief of repression by YcgE, which is further enhanced by blue light irradiation (*13*). They found that YcgF and YcgE expressions are strongly activated at low temperatures. Therefore, the overexpression of YcgF can explain the increased relief of repression. In this study, we found the possibility showing that the YcgF affinity (interprotein interaction) for YcgE is increased by both lowering temperature and light irradiation. It suggests that YcgF itself plays a role of the thermometer as well as blue light sensor in a molecular level. The temperature-sensitive YcgF affinity may be responsible for a rapid response to a change of temperature. To give a deeper insight, it is interesting to detect the interaction between YcgF and YcgE directly by using the TG method, which will be a future study.

Recently, on the basis of the temperature-dependent lifetime of the light-adapted state of YcgF, it was suggested that YcgF could possess a function as a thermometer (*22*). However, the rates of most of chemical reactions depend on temperature so the temperature-dependent lifetime does not necessarily mean the protein behaves as a temperature sensor. We believe that the temperature-dependent equilibrium of the reactive and nonreactive species of YcgF is more conclusive evidence of YcgF acting as a temperature sensor.

A similar temperature-dependent equilibrium was observed for another class of blue light sensor proteins, a LOV protein, phototropin, in which a single α-helix (Jα) joins the photoreceptive LOV2 domain to a protein kinase effector domain. An NMR study and TG experiment found that blue light irradiation leads to disruption of the J-helix of phot1 LOV2 against the outer face of the central $\beta$-sheet of the LOV2 core, which should be an essential step for the function (*44*−*46*). For this protein, it was shown that there is an equilibrium between the photoreactive and nonreactive forms in the dark state, and the equilibrium constant is temperature dependent (*47*, *48*). This example indicates that other photosensor proteins could function as temperature sensors as well as YcgF.

## SUPPORTING INFORMATION AVAILABLE

Principles and theory of the measurements, analysis of equilibrium between monomer and dimer, analysis of volume change, and temperature-dependent volume change. This

material is available free of charge via the Internet at http://pubs.acs.org.

## REFERENCES


1. Rajagopal, S., Key, J. M., Purcell, E. B., Boerema, D. J., and Moffat, K. (2004) Purification and initial characterization of a putative blue light-regulated phosphodiesterase from *Escherichia coli*. *Photochem. Photobiol. 80*, 542–547.
2. Masuda, S., and Ono, T. (2005) Comparative spectroscopic studies of sensor of blue-light using FAD (BLUF) proteins. AppA of *Rhodobacter sphaeroides* and YcgF of *Escherichia coli*, in Photosynthesis: Fundamental Aspects to Global Perspectives (van der Est, A., and Bruce, D., Eds.) Vol. *2*, pp 700−702, Allen Press, Lawrence, KS.
3. van der Horst, M. A., and Hellingwerf, K. J. (2004) Photoreceptor proteins, "star actors of modern times": a review of the functional dynamics in the structure of representative members of six different photoreceptor families. *Acc. Chem. Res. 37*, 13–20.
4. Gomelsky, M., and Klug, G. (2002) BLUF: a novel FAD-binding domain involved in sensory transduction in microorganisms. *Trends Biol. Sci. 27*, 497–500.
5. Masuda, S., and Bauer, C. E. (2002) AppA is a blue light photoreceptor that antirepresses photosynthesis gene expression in *Rhodobacter sphaeroides*. *Cell 110*, 613–623.
6. Braatsch, S., Gomelsky, M., Kuphal, S., and Klug, G. (2002) A single flavoprotein, AppA, integrates both redox and light signals in *Rhodobacter sphaeroides*. *Mol. Microbiol. 45*, 827–836.
7. Masuda, S., Hasegawa, K., Ishii, A., and Ono, T. (2004) Light-induced structural changes in a putative blue-light receptor with a novel FAD binding fold sensor of blue-light using FAD (BULF); Slr1694 of *Synechocystis* sp. PCC6803. *Biochemistry 43*, 5304–5313.
8. Iseki, M., Matsunaga, S., Murakami, A., Ohno, K., Shiga, K., Yoshida, K., Sugai, M., Takahashi, T., Hori, T., and Watanabe, M. (2002) A blue-light-activated adenylyl cyclase mediates photoavoidanse in *Euglena gracilis*. *Nature 415*, 1047–1051.
9. Fukushima, Y., Okajima, K., Shibata, Y., Ikeuchi, M., and Itoh, S. (2005) Primary intermediate in the photocycle of a blue-light sensory BLUF FAD-protein, Tll0078, of *Thermosynechococcus elongatus* BP-1. *Biochemistry 44*, 5149–5158.
10. Kita, A., Okajima, K., Morimoto, Y., Ikeuchi, M., and Miki, K. (2005) Structure of a cyanobacterial BLUF protein, Tll0078, containing a novel FAD-binding blue-light sensor domain. *J. Mol. Biol. 349*, 1–9.
11. Jung, A., Domratcheva, T., Tarutina, M., Wu, Q., Ko, W-h., Shoeman, R. L., Gomelsky, M., Gardner, K. H., and Schlichting, I. (2005) Structure of a bacterial BLUF photoreceptor: insights into blue-mediated signal transduction. *Proc. Natl. Acad. Sci. U.S.A. 101*, 12306–12311.
12. Yuan, H., Anderson, S., Masuda, S., Dragnea, V., Moffat, K., and Bauer, C. (2006) Crystal structures of the *Synechocystis* photoreceptor Slr1694 reveal distinct structural states related to signaling. *Biochemistry 45*, 12687–12694.
13. Tschowri, N., Busse, S., and Hengge, R. (2009) The BLUF-EAL protein YcgF acts as a direct anti-repressor in a blue-light response of *Escherichia coli*. *Genes Dev. 15*, 522–534.
14. Ito, S., Murakami, A., Sato, K., Nishina, Y., Shiga, K., Takahashi, T., Higashi, S., Iseki, M., and Watanabe, M. (2005) Photocycle features of heterologously expressed and assembled eukaryotic flavin-binding BLUF domains of photoactivated adenylyl cyclase (PAC), a blue-light receptor in *Euglena gracilis*. *Photochem. Photobiol. Sci. 4*, 762–769.
15. Masuda, S., Hasegawa, K., and Ono, T. (2005) Light-induced structural changes of apoprotein and chromophore in the sensor of blue light using FAD (BLUF) domain of AppA for a signaling state. *Biochemistry 44*, 1215–1224.
16. Anderson, S., Dragnea, V., Masuda, S., Ybe, J., Moffat, K., and Bauer, C. E. (2005) Structure of a novel photoreceptor, the BLUF domain of AppA from *Rhodobacter sphaeroides*. *Biochemistry 44*, 7998–8005.
17. Jung, A., Reinstein, J., Domratcheva, T., Shoeman, R. L., and Schlichting, I. (2006) Crystal structures of the AppA BLUF domain photoreceptor provide insights into blue light-mediated signal transduction. *J. Mol. Biol. 362*, 717–732.
18. Gauden, M., Yeremenko, S., Laan, W., van Stokkum, I. H. M., Ihalainen, J. A., van Grondelle, R., Hellingwerf, K. J., and Kennis, T. M. (2005) Photocycle of the flavin-binding photoreceptor AppA, a bacterial transcriptional antirepressor of photosynthetic genes. *Biochemistry 44*, 3653–3662.
19. Unno, M., Sano, R., Masuda, S., Ono, T., and Yamauchi, S. (2005) Light-induced structural changes in the active site of the BLUF domain in AppA by Raman spectroscopy. *J. Phys. Chem. B 109*, 12620–12626.
20. Hasegawa, K., Masuda, S., and Ono, T. (2006) Light induced structural changes of a full-length protein and its BLUF domain in YcgF(Blrp), a blue-light sensing protein that uses FAD (BLUF). *Biochemistry 45*, 3785–3793.
21. Nakasone, Y., Ono, T. A., Ishii, A., Masuda, S., and Terazima, M. (2007) Transient dimerization and conformational change of a BLUF protein: YcgF. *J. Am. Chem. Soc. 129*, 7028–7035.
22. Schroeder, C., Werner, K., Otten, H., Krätzig, S., Schwalbe, H., and Essen, L. O. (2008) Influence of a joining helix on the BLUF domain of the YcgF photoreceptor from *Escherichia coli*. *ChemBioChem 9*, 2463–2473.
23. Terazima, M., Okamoto, K., and Hirota, N. (1995) Translational diffusion of transient radicals created by the photoinduced hydrogen abstraction reaction in solution: anomalous size dependence in the radical diffusion. *J. Chem. Phys. 102*, 2506–2512.
24. Terazima, M. (2000) Is the translational diffusion of organic radicals different from that of closed-shell molecules? *Acc. Chem. Res. 33*, 687–694.
25. Takeshita, K., Imamoto, Y., Kataoka, M., Mihara, K., Tokunaga, F., and Terazima, M. (2002) Structural change of site-directed mutants of PYP: new dynamics during pR state. *Biophys. J. 83*, 1567–1577.
26. Nada, T., and Terazima, M. (2003) A novel method for study of protein folding kinetics by monitoring diffusion coefficient in time domain. *Biophys. J. 85*, 1876–1881.
27. Inoue, K., Sasaki, J., Morisaki, M., Tokunaga, F., and Terazima, M. (2004) Time-resolved detection of sensory rhodopsin II-transducer interaction. *Biophys. J. 87*, 2587–2597.
28. Terazima, M. (2006) Diffusion coefficients as a monitor of reaction kinetics of biological molecules. *Phys. Chem. Chem. Phys. 8*, 545–557.
29. Hazra, P., Inoue, K., Laan, W., Hellingwerf, K. J., and Terazima, M. (2006) Tetramer formation kinetics in the signaling state of AppA monitored by time-resolved diffusion. *Biophys. J. 91*, 654–661.
30. Nakasone, Y., Eitoku, T., Matsuoka, D., Tokutomi, S., and Terazima, M. (2006) Kinetic measurement of transient dimerization and dissociation reactions of *Arabidopsis* phototropin 1 LOV2 domain. *Biophys. J. 91*, 645–653.
31. Eitoku, T., Nakasone, Y., Zikihara, K., Matsuoka, D., Tokutomi, S., and Terazima, M. (2007) Photochemical intermediates of Arabidopsis phototropin 2 LOV domains associated with conformational changes. *J. Mol. Biol. 371*, 1290–1303.
32. Salamat-Miller, N., Chittchang, M., Mitra, A. K., and Johnston, T. P. (2002) Shape imposed by secondary structure of a polypeptide affects its free diffusion through liquid-filled pores. *Int. J. Pharm. 244*, 1–8.
33. Van Holde, K. E., Johnson, W. C., and Shing Ho, P. (1998) Physical Biochemistry, Prentice-Hall, Englewood Cliffs, NJ.
34. Wu, Q., Ko, W. H., and Gardner, K. H. (2008) Structural requirements for key residues and auxiliary portions of a BLUF domain. *Biochemistry 47*, 10271–10280.
35. Wu, Q., and Gardner, K. H. (2009) Structure and insight into blue light-induced changes in the BlrP1 BLUF domain. *Biochemistry 48*, 2620–2629.
36. Buttani, V., Losi, A., Eggert, T., Krauss, U., Jaeger, K. E., Cao, Z., and Gärtner, W. (2007) Conformational analysis of the blue-light sensing protein YtvA reveals a competitive interface for LOV-LOV dimerization and interdomain interactions. *Photochem. Photobiol. Sci. 6*, 41–49.
37. Jaenicke, E., Walsh, P. J., and Decker, H. (2003) Isolation and characterization of haemoporin, an abundant haemolymph protein from *Aplysia californica*. *Biochem. J. 375*, 681–688.
38. Landau, L., and Lifschitz, E. (1969) Statistical Physics, Theoretical Physics 5, Pergamon Press, Oxford.
39. Heremans, K., and Smeller, L. (1998) Protein structure and dynamics at high pressure. *Biochim. Biophys. Acta 1386*, 353–370.
40. Zipp, A., and Kauzmann, W. (1973) Pressure denaturation of metmyoglobin. *Biochemistry 12*, 4217–4228.
41. Yuan, H., and Bauer, C. E. (2008) PixE promotes dark oligomerization of the BLUF photoreceptor PixD. *Proc. Natl. Acad. Sci. U.S.A. 105*, 11715–11719.
42. Tanaka, K., Nakasone, Y., Okajima, K., Ikeuchi, M., Tokutomi, S., and Terazima, M. (2009) Oligomeric-state-dependent conformational change of the BLUF protein TePixD (Tll0078). *J. Mol. Biol. 386*, 1290–1300.
43. Barends, T. R., Hartmann, E., Griese, J. J., Beitlich, T., Kirienko, N. V., Ryjenkov, D. A., Reinstein, J., Shoeman, R. L., Gomelsky, M., and Schlichting, I. (2009) Structure and mechanism of a bacterial

light-regulated cyclic nucleotide phosphodiesterase. *Nature 459*, 1015–1018.
44. Harper, S. M., Neil, L. C., and Gardner, K. H. (2003) Structural basis of a phototropin light switch. *Science 301*, 1541–1544.
45. Harper, S. M., Christie, J. M., and Gardner, K. H. (2004) Disruption of the LOV-Jalpha helix interaction activates phototropin kinase activity. *Biochemistry 43*, 16184–16192.
46. Nakasone, Y., Eitoku, T., Matsuoka, D., Tokutomi, S., and Terazima, M. (2007) Dynamics of conformational changes of *Arabidopsis* phototropin 1 LOV2 with the linker domain. *J. Mol. Biol. 367*, 432–442.
47. Yao, X., Rosen, M. K., and Gardner, K. H. (2008) Estimation of the available free energy in a LOV2-J alpha photoswitch. *Nat. Chem. Biol. 4*, 491–497.
48. Nakasone, Y., Eitoku, T., Zikihara, K., Matsuoka, D., Tokutomi, S., and Terazima, M. (2008) Stability of dimer and domain-domain interaction of *Arabidopsis* phototropin 1 LOV2. *J. Mol. Biol. 383l*, 904–913.